Adsorption of O, OH, and H 2 O on Pt−Based Bimetallic Clusters Alloyed with Co, Cr, and Ni

ARTICLE *in* THE JOURNAL OF PHYSICAL CHEMISTRY A · JULY 2004

Impact Factor: 2.69 · DOI: 10.1021/jp0489572

6 AUTHORS, INCLUDING:

Perla B. Balbuena
Texas A&M University
245 PUBLICATIONS **5,781** CITATIONS
SEE PROFILE

Diego Altomare
University of South Carolina
20 PUBLICATIONS **153** CITATIONS
SEE PROFILE

Jorge Seminario
Texas A&M University
232 PUBLICATIONS **4,953** CITATIONS
SEE PROFILE

Adsorption of O, OH, and H_2O on Pt-Based Bimetallic Clusters Alloyed with Co, Cr, and Ni

Perla B. Balbuena,*,†,§ Diego Altomare,† Nagendra Vadlamani,‡ Sridhar Bingi,‡ Luis A. Agapito,‡ and Jorge M. Seminario*,‡,§

Department of Chemical Engineering, University of South Carolina, Columbia, South Carolina 29208, and Department of Electrical Engineering, University of South Carolina, Columbia, South Carolina 29208

Received: March 8, 2004; In Final Form: May 15, 2004

Binding energies and preferred adsorption sites of O, OH, and H_2O to bimetallic clusters PtX, Pt_2X, and PtX_2 (X = Pt, Co, Cr, Ni) are determined using density functional theory. The second metal element in the alloy has stronger affinity for OH than the Pt sites, and it is able to adsorb up to two OH radicals per site in oxygenated clusters. The highest binding strength of atomic oxygen is found in the hollow sites of Ni_3 and Co_3, followed by adsorption in hollow or bridge sites of Pt_2X or PtX_2, in all cases significantly stronger than that found in Pt_3. H_2O adsorbs on top sites of pure and alloy clusters with much weaker energies compared with those of OH and O; however, the H_2O binding strength in the Co, Cr, and Ni atoms is enhanced with respect to that on the Pt site, whereas the binding strength of H_2O on the top of Pt sites of the alloy clusters is much reduced with respect to that in the pure cluster.

1. Introduction

Pt-based bimetallic nanoclusters alloyed with Co, Cr, and Ni are potential candidate materials for electrocatalysts of oxygen electroreduction (OER) in an acid medium, where intermediate species and reaction products include adsorbed O, OH, and H_2O. Experimental work[1−5] indicated that effective alloys made with Pt−Co, Pt−Cr, and Pt−Ni are at least as good as pure Pt, and in many cases, the alloyed material showed a better performance for the O_2 electroreduction; the reasons for such behavior are still debated.[1,3−6]

Details about the mechanism of oxygen electroreduction are controversial.[7] Theoretical work suggests that the first electron transfer involves protonation of O_2 near to the surface[8−10] yielding an end-on adsorption mode for H−O−O, followed by dissociation of the O−O bond and adsorption of OH and O, and successive electron and proton transfers lead to adsorbed water.[7,11,12] Our recent work[6] demonstrated that ensembles containing XPt and XXPt (X = Co or Cr) are the best active sites to promote O_2 dissociation. Dynamic Monte Carlo simulations[13] of the OER assuming a four-electron reaction concluded that water coverage of the surface limits the oxygen adsorption and reduces the magnitude of the current at intermediate overpotentials. On the other hand, recent experimental[12] and theoretical[14] works suggest that adsorbed OH poisons the Pt electrode and is one of the causes of overpotential in the oxygen electroreduction reaction in acid medium.

Since the four-electron O_2 dissociation process in acid medium starts from O_2 adsorption on the catalytic surface and the presence of other adsorbed species may interfere in various ways with this process,[2,5,6] understanding the nature and relative magnitude of adsorption of the main intermediate species on the various bimetallic ensembles is crucial to the first-principles design of alternative catalysts. Bimetallic mixtures exhibit the well-known surface segregation phenomena, where the component with the lowest surface energy may preferentially occupy surface sites.[15] In nanoclusters, the phenomena becomes more complex because of the existence of several different types of sites (edges, corners, terraces, steps, and regular surface sites), which due to their geometry may have peculiar electronic characteristics.[16,17] In previous work, we have examined surface segregation in several bimetallic nanocluster systems and reported their atomic distribution using molecular dynamics simulations and many-body potentials for the metal−metal interactions.[18,19] We emphasize that in real catalysts such atomic distribution depends strongly on the fabrication method, and therefore, the nanocluster structure and exposed surfaces do not always correspond to thermodynamic stable phases. Our main interest is to analyze most of the possible bimetallic ensembles constituted by a few atoms that may act as the active sites of the exposed surfaces and to present a *comparative* study about their binding properties with respect to the intermediate species of the OER. We recognize that quantum size effects exist in these small systems, as reported in previous publications;[20−23] however, our conclusions are based on the *comparative* behavior of bimetallic systems for a fixed cluster size. Thus, we investigate adsorption of O, OH, and water in PtXPt and PtXX systems (with X = Co, Cr, and Ni), identifying the most stable structures and binding sites. Finally, we examine the possibility of adsorption of more than one OH species to a top site of oxygenated bimetallic clusters. These results are critically evaluated to assess the effect of the adsorption of intermediate species on the oxygen dissociation in bimetallic surfaces. We intend to provide a useful guide for understanding which designs would be the most favorable for the OER and possibly offer a rational criterion to modify some catalyst fabrication procedures.

2. Methodology

Density functional theory (DFT) is used to determine optimized structures and binding energies for the various metallic

* To whom correspondence may be addressed. E-mail: balbuena@engr.sc.edu (P.B.B.); jsemina@engr.sc.edu (J.M.S.).
† Department of Chemical Engineering.
‡ Department of Electrical Engineering.
§ Current address: Department of Chemical Engineering, Texas A&M University, College Station, TX 78743.

10.1021/jp0489572 CCC: $27.50
Published on Web 07/02/2004

TABLE 1: OH Binding Energies to Pt-Based Clusters, Multiplicities of the Ground States, Total Energies, and OH Adsorption Site[a]

system	multiplicity	adsorption site	energy (Ha)	−BE (eV)
OHPtPtPt	4	bridge Pt−Pt	−433.33202	2.10
OHPtPtPt	2	top	−433.36217	2.92
OHPtPtCr	6	top of Pt	−400.53671	2.90
OHCrPtPt	4	top of Cr	−400.56166	3.58
OHPtCrCr	2	top of Pt	−367.65602	3.32
OHCrCrPt	2	bridge Cr−Cr	−367.71366	4.89
OHPtPtNi	4	top of Pt	−483.52405	3.13
OHNiPtPt	2	top of Ni	−483.52193	3.07
OHPtNiNi	4	top of Pt	−533.65122	2.74
OHNiNiPt	2	bridge Ni−Ni	−533.69283	3.88
OHPtCoPt	5	top of Pt	−459.29483	2.94
OHCoPtPt	5	top of Co	−459.31759	3.56
OHPtCoCo	6	top of Pt	−485.18509	2.88
OHCoCoPt	6	bridge Co−Co	−485.23803	4.32
OHPtPt	2	top	−314.11330	2.79
OHCrPt	6	top of Cr	−281.31929	3.29
OHCrCr	2	top	−248.45785	6.11
OHPtNi	2	bridge Pt−Ni	−364.29183	4.36
OHNiNi	4	bridge Ni−Ni	−414.42764	3.79
OHCoPt	3	top of Co	−340.07998	4.17
OHCoCo	6	bridge Co−Co	−365.96646	3.20

[a] The B3PW91 functional is used for all calculations with the LANL basis set and effective core potential for the metals and the full electron 6-31G(d) basis set for O and H atoms.

clusters and their complexes with O, OH, and H_2O. All possible spin multiplicities are investigated to determine the lowest-energy configurations, and second derivatives of the total energy are calculated to determine the stability of the structures. No restrictions were imposed for optimizations. The 2-fold bridge, 1-fold top, and 3-fold hollow adsorption sites are tested as initial configurations for all cases. We compare adsorption strengths among several different alloy ensembles involving Pt as the central element. For consistency with our previous studies,[6] we use the B3PW91 hybrid functional[24−26] with the effective core potential and basis set LANL2DZ[27−29] for all metal atoms, and the full-electron basis set 6-31G*[30] for O and H. The B3PW91 procedure consists of the Becke3 hybrid exchange functional combined with the generalized gradient approximation (GGA) Perdew−Wang91 correlation.[25,31] Currently, DFT using hybrid exchange and GGA correlation functionals are the most powerful tools to deal with metal−small molecule systems.[22,32,33] The LANL2DZ explicitly considers all the valence electrons rather than just those in the last electronic shell. Core electrons are treated in an approximate way using pseudopotentials that include relativistic effects allowing an excellent account of heavy metal atoms.[27] The B3PW91/LANL2DZ level of theory has been previously used in other works where further details can be found.[6,20,23] The calculations are performed with the program Gaussian 98.[34]

3. Results and Discussion

3.1. OH Adsorption. Binding energies (BE) corresponding to the most stable (lowest-energy) geometrical arrangements of OH adsorbed on PtPtPt, PtPtX, and PtXX (X = Cr, Co, and Ni) are reported in the first part of Table 1. BEs are defined from the reaction

$$\text{adsorbate} + \text{metallic cluster} \rightarrow \text{complex}$$

The first two rows of Table 1 indicate a preference for the "on top" adsorption of OH on a pure Pt cluster over the bridge site adsorption. All three types of adsorption, on top,[35,36] bridge,[36] and hollow,[37−39] have been reported from experimental observations of OH adsorption on Pt(111). Bridge and top adsorption were found as the most favorable sites at low coverages.[36] Moreover, recent ab initio MD simulations[9] indicate that diffusion from top to bridge is highly probable, although, in the presence of water, OH adsorbed on top sites seems to be stabilized by H bonding to neighbor (nonadsorbed) water molecules from the electrolyte.[9,36]

Binding energies from Table 1 show that when Cr substitutes one of the Pt atoms (PtPtCr), OH adsorbs preferentially on top of the Cr site, whereas when two Pt atoms are substituted, in PtCrCr, a strong preference is found for adsorption on the bridge CrCr site. Exactly the same trends are observed for Co and Ni in the PtXX clusters, i.e., OH prefers to adsorb on the XX bridge site; the order of adsorption strength is Cr > Co > Ni. The BE of OH on top of a Pt atom is very sensitive to the nature of the atomic environment surrounding Pt. For example, the BE of OH to a top Pt site in PtPtPt is −2.92 eV, whereas it is −3.32 eV in PtCrCr, −2.94 eV in PtCoCo, and −2.74 eV in PtNiNi. In agreement with our results, other DFT calculations had reported a relative adsorption strength of top > bridge > hollow for OH adsorbed on Pt(111).[36,39] Our calculated Pt−O distances are 0.1 Å shorter than those obtained by DFT on extended surfaces, whereas our calculated OH bond in the adsorbed OH is 0.97 Å compared to 0.98 Å found by Koper et al.[39] The tilted mode found for OH adsorption on top sites agrees well with experimental findings.[37]

In all cases, the foreign atom (Cr, Co, Ni) becomes highly oxidized, as shown by their positive atomic Mulliken charges[40−42] (not shown), which causes a strong electrostatic interaction with the negatively charged O of the adsorbed hydroxyl group, OH_{ads}. We emphasize that the electronic charges are not physical observables, but their estimation provides a rough description of the electronic density. Such a charge-transfer effect is also detected in the PtPtX clusters, where OH prefers to adsorb on top of Co (Cr) to on top of Pt. However, for X = Ni, OH still prefers to adsorb on top of Pt, although the difference in BE is only 0.06 eV. Thus, although the oxidation of Ni is clearly observed, these results do not support the speculation that in the OER the Ni atoms would act as sacrificial sites where OH could be adsorbed preferentially, with the only exception of adsorption on the Ni−Ni bridge site. In a later section, we address this point further in relation to H_2O adsorption.

Table 2 illustrates the relative stability of the ground states with respect to their closest local minima. The spin multiplicities corresponding to the lowest-energy structures are generally high, as expected for complexes involving transition metals, and in some cases, there are states with very similar energies such as the doublet and quartet of OHPtPtPt and those of OHNiPtPt.

3.2. O Adsorption. Results of binding energies for the adsorption of atomic oxygen on PtPtPt, PtXX, and PtPtX and on PtPt and PtX dimers are presented in Table 3. Stable O adsorption is found on the bridge site of Pt_3, in agreement with previous studies,[23] with a BE of −3.24 eV, much weaker than the adsorption strength in hollow sites of Ni_3 (−5.01 eV) and Co_3 (−4.97 eV). Other theoretical[43] and experimental[44,45] studies have reported adsorption of atomic oxygen in hollow sites on Pt(111) surfaces with average adsorption energies of 3.7 eV and about 0.2−0.3 eV less strong adsorption on bridge sites.[46] In the PtXX complexes, with X = Co or Ni, adsorption of O in the hollow site is preferred to that on the XX bridge site. In both cases, hollow and bridge, the adsorption strength is always higher than in Pt_3. If only one foreign atom is present, such as the case of PtPtCo, the O atoms prefers to adsorb on the PtCo

TABLE 2: Energy Differences (in eV) between the Ground State and Higher-Energy States for the Systems in Table 1[a]

	m							
system	1	2	3	4	5	6	7	8
OHPtPtCr (t)		1.46		1.36		0		0.36
OHCrPtPt (t)		1.00		0		0.16		
OHPtCrCr (t)		0		1.66		2.24		
OHCrCrPt (b)		0		1.30		1.70		
OHPtPtPt (b)		0.11		0		1.53		
OHPtPtPt (t)		0		0.04		1.33		
OHPtPtNi (t)		0.38		0		1.24		
OHNiPtPt (t)		0		0.01		1.02		
OHPtNiNi (t)		0.17		0		0.59		
OHNiNiPt (b)		0		0.13				
OHPtCoCo (t)		0.18		0.88		0		0.14
OHCoCoPt (b)		0.29		1.00		0		1.83
OHPtCoPt (t)	2.39		0.60		0		2.04	
OHCoPtPt (t)	1.75		0.86		0		0.61	
OHCrPt (t)		1.00		0.23		0		1.28
OHPtNi (b)		0		0.44		1.90		
OHCoPt (t)	2.60		0		0.79			
OHCrCr (b)		0		1.63		2.17		
OHCoCo (b)		0.02		0.70		0		0.53
OHPtPt (t)		0		0.27		2.48		
OHNiNi (b)		0.02		0		0.93		

[a] The adsorption site is indicated within parentheses as t = top, b = bridge.

TABLE 3: O Binding Energies to Pt-Based Clusters, Multiplicities of the Ground States, Total Energies, and O Adsorption Site[a]

system	multiplicity	adsorption site	energy (Ha)	−BE (eV)
OPtPtPt	3	bridge	−432.71093	3.24
OPtCoPt	4	bridge Pt−Co	−458.66596	3.87
OPtCoPt	2	hollow	−458.63526	3.03
OPtCoCo	5	hollow	−484.55999	3.90
OCoCoPt	1	bridge Co−Co	−484.48538	1.88
OCoCoCo	4	hollow	−510.46448	4.97
OPtCrPt	5	bridge Pt−Cr	−399.91737	4.09
OPtCrCr	5	top of Cr	−367.05407	4.98
OCrCrPt	7	bridge Cr−Cr	−367.02357	4.15
OPtPtNi	3	hollow	−482.86969	3.36
OPtNiPt	1	bridge Pt−Ni	−482.86483	3.23
OPtNiNi	3	hollow	−533.03424	3.99
ONiNiPt	5	bridge Ni−Ni	−533.01961	3.60
ONiNiNi	3	hollow	−583.17573	5.01
OPtPt	1	bridge	−313.45774	2.99
OPtCo	4	top of Co	−339.43337	4.61
OPtCr	3	top of Cr	−280.69033	4.21
OPtNi	3	bridge	−363.66317	3.95
OCoCo	5	bridge	−365.34910	4.44
OCrCr	3	top of Cr	−247.81482	6.65
ONiNi	3	bridge	−413.81139	5.06

[a] The B3PW91 functional is used for all calculations with the LANL basis set and effective core potential for the metals and the full electron 6-31G(d) basis set for O and H atoms.

bridge site instead of in the hollow site, whereas in PtPtNi, the hollow site is preferred to the PtNi bridge site (although the energy difference is 0.13 eV). Adsorption on top of the Cr site is preferred in the PtPtCr clusters, followed by adsorption on top of the Pt atom.

In the PtCrCr clusters, adsorption at the CrCr bridge site is stronger than that on top of the Pt atom. Overall, we observe a strong affinity for atomic oxygen in hollow sites of pure Ni and Co clusters. This affinity (as discussed for OH adsorption) shows the tendency to oxidation of such metal atoms. In addition, high adsorption strengths are found on the bridge PtX sites (X = Co and Ni) and on top of the Cr sites. Such strong chemisorption resulting from oxidation of Co, Cr, and Ni sites would not be favorable for the OER, because the surface would become poisoned with unwanted strongly adsorbed species, unless the subsequent reduction processes would yield products with associated low barrier desorption processes. All these complexities require including the adsorption/desorption of H_2O and OH in the analysis.

TABLE 4: Energy Differences (in eV) between the Ground State and Higher-Energy States for the Systems in Table 3[a]

	m						
system	1	2	3	4	5	6	7
OPtPtPt (b)	0.02		0		0.82		
OPtCoPt (b)		0.84		0		0.94	
OPtCoCo (h)	2.03		0.28		0		0.07
OCoCoCo (h)		0.10		0	0.33		
OPtCrPt (b)	0.75		0.92		0		0.81
OPtCrCr (t)	4.38		1.29		0		0.83
OPtPtNi (h)	0.13		0		0.29		1.56
OPtNiNi (h)	0.61		0		0.40		1.52
ONiNiNi (h)	1.77		0		0.27		
OPtPt (b)	0		0.82		0.48		
OPtCo (b)		0.34		0		0.72	
OPtCr (t)	2.85		0		0.51		
OPtNi (b)	0.52		0		0.92		2.75
OCoCo (b)	3.51		0.47		0		0.16
OCrCr (t)	4.70		0		0.83		
ONiNi (b)	0.95		0		0.54		1.99

[a] The adsorption site is indicated within parentheses as t = top, b = bridge, h = hollow.

Table 4 shows energy differences between the ground state and its closest local minima energy states of different spin multiplicities. Except for the singlet and triplet of OPt_3 (separated only by 0.02 eV) and the quintet and septet of OPtCoCo (separated by 0.07 eV), considerable energy differences are found for the other cases indicating that the ground states are highly stable.

3.3. H_2O Adsorption. Much weaker energies (relative to the OH and O adsorption) are found for adsorption of a H_2O molecule on the clusters, as shown in Table 5. In all cases, the preferred site is on top, in agreement with previous reports.[47,48] The Pt−O distance in Pt_3 is 2.22 Å, compared to a value of 2.43 Å reported by Meng at al.[47] from ab initio molecular dynamics simulations. On the PtPtCr cluster, H_2O adsorbs on top of the Cr atom with the same strength as in Pt_3 (−1.02 eV); however, the BE to adsorb on top of Pt is reduced by 0.21 eV, whereas in the PtCrCr cluster, the preferred adsorption is again on top of one of the Cr atoms, but the adsorption on top of Pt is significantly lowered to −0.39 eV. A relatively weak adsorption (BE = −0.58 eV) is found on a top site of a CrCrCr ensemble. For the Ni-containing clusters, we found a relatively strong adsorption of H_2O on top of the Ni atom in PtPtNi and slightly lower in PtNiNi. Similar to the case of PtCrCr, the adsorption of H_2O on top of Pt in the PtNiNi ensemble is very weak (−0.12 eV). In contrast to the OH adsorption, these results support the idea of Ni acting as "sacrificial sites" that would adsorb H_2O on atoms other than Pt. This interesting result implies that it would be possible to design catalysts at reduced costs, keeping the efficiency of pure Pt, provided that enough Pt surface atoms are available as in high surface area nanoparticles.

A similar phenomenon is found in the Co-containing clusters; the binding strength of H_2O on top of Co atoms is equivalent to the one in the Pt_3 cluster (−1.06 eV in PtPtCo and −0.97 eV in PtCoCo), whereas the adsorption energy on top of the Pt atom in both clusters is lowered to −0.86 in PtPtCo and −0.69 eV in PtCoCo. Adsorption on dimer clusters is also included in Table 5 for completeness. The differences in energies between

TABLE 5: H_2O Binding Energies to Pt-Based Clusters, Multiplicities of the Ground States, Total Energies, and OH Adsorption Site[a]

system	multiplicity	adsorption site	energy (Ha)	−BE (eV)
$H_2O-PtPtPt$	1	top	−433.97948	1.02
$H_2O-CrPtPt$	5	top of Cr	−401.15470	1.02
$H_2O-PtPtCr$	5	top of Pt	−401.14705	0.81
$H_2O-CrCrPt$	3	top of Cr	−368.26006	1.05
$H_2O-PtCrCr$	3	top of Pt	−368.23566	0.39
$H_2O-CrCrCr$	7	top	−335.37532	0.58
$H_2O-PtPtNi$	3	top of Ni	−484.14234	1.25
$H_2O-NiNiPt$	3	top of Ni	−534.27329	0.97
$H_2O-PtNiNi$	5	top of Pt	−534.24201	0.12
$H_2O-NiNiNi$	5	top	−584.37528	0.91
$H_2O-PtCoCo$	5	top of Co	−485.80246	0.97
$H_2O-CoCoPt$	5	top of Pt	−485.79205	0.69
$H_2O-PtPtCo$	4	top of Co	−459.91305	1.06
$H_2O-PtPtCo$	4	top of Pt	−459.90574	0.86
$H_2O-CoCoCo$	8	top	−511.66394	0.87
$H_2O-PtPt$	3	top	−314.75062	1.43
$H_2O-CrPt$	7	top of Cr	−281.91524	0.80
$H_2O-PtCr$	7	top of Pt	−281.89107	0.14
$H_2O-CrCr$	3	top	−248.99122	1.93
$H_2O-NiPt$	3	top of Ni	−364.90839	2.44
$H_2O-PtNi$	3	top of Pt	−364.89376	2.04
$H_2O-NiNi$	3	top	−415.03927	1.73
$H_2O-CoPt$	4	top of Co	−340.67938	1.78
$H_2O-PtCo$	4	top of Pt	−340.66515	1.39
$H_2O-CoCo$	5	top	−366.56202	0.71

[a] The B3PW91 functional is used for all calculations with the LANL basis set and effective core potential for the metals and the full electron 6-31G(d) basis set for O and H atoms.

TABLE 6: Energy Differences (in eV) between the Ground State and Higher-Energy States for Systems in Table 5[a]

	m									
system	1	2	3	4	5	6	7	8	9	10
$H_2O-CrPtPt$	3.18		0.41		0		0.27			
$H_2O-PtPtCr$	3.34		1.45		0		0.06			
$H_2O-CrCrPt$	4.34		0		2.99					
$H_2O-PtCrCr$	3.72		0		1.35					
$H_2O-PtPtPt$	0		0.03		0.85					
$H_2O-PtPtNi$	0.64		0		0.47					
$H_2O-NiNiPt$	1.25		0		0.36					
$H_2O-PtNiNi$	0.84		0.18		0		1.28			
$H_2O-PtCoCo$	3.68		0.76		0		0.13			
$H_2O-PtPtCo$		0.48		0		0.74				
$H_2O-PtPtCo$		1.28		0		0.23				
$H_2O-CrCrCr$	8.49		2.36		0.44		0		1.54	
$H_2O-NiNiNi$	1.80		0.05		0		1.58			
$H_2O-CoCoCo$		1.64		1.77		0.20		0		0.66
$H_2O-CrPt$	3.21		1.47		0.07		0		2.19	
$H_2O-NiPt$	1.00		0		1.48					
$H_2O-PtNi$			0							
$H_2O-CoPt$		0.24		0		1.24				
$H_2O-PtCo$		0.41		0		1.07				
$H_2O-CrCr$	3.50		0		1.34					
$H_2O-CoCo$	4.18		0.77		0		0.86			
$H_2O-PtPt$	0.58		0		1.74					
$H_2O-NiNi$	1.97		0		1.28					

[a] In all cases, for a cluster XYZ or XY, water is adsorbed with the oxygen atom on top of the metal atom X.

the ground state and closest excited states displayed in Table 6 show that most energy differences are relatively large, implying stable ground states.

In summary, the important result in relation to the OER is the significant lowering of the binding energy of H_2O to the Pt sites, when they are surrounded by foreign atoms such as Cr, Co, and Ni.

3.4. Adsorption of More Than One OH Radical to A Site of Oxygenated Metallic Clusters. As mentioned in the Introduction, it is speculated that OH adsorption negatively affects the efficiency of the OER on Pt-based surfaces,[12,14] occupying sites that otherwise could be used to adsorb and reduce O_2 and consequently reducing the net electroreduction current. For this reason, we have tested the affinity for OH of the metallic atoms in O_2PtPtX, O_2PtXPt, O_2PtXX, and O_2XXPt. O_2XYZ means that O_2 is adsorbed on the XY bridge site. Adsorption of one and two OH groups is successively tested in all the oxygenated clusters, as shown in Table 7. The total energies and zero-point energies of the lowest-energy state for the neutrals of all systems considered and their corresponding multiplicities are listed in Table 8, and those of the anions are listed in Table 9. Second-derivative calculations yielding non-negative eigenvalues of the Hessian matrix show that the systems correspond to local minima. The energies of several possible spin states with respect to the ground state energy are summarized in Table 10. OH adsorption to oxygenated clusters (Table 9) follow the same trends found for adsorption in the corresponding nonoxygenated clusters reported in Table 1, i.e., adsorption on top of Cr, Ni, or Co is preferred to adsorption on the Pt site of the same PtXX cluster. However, in most cases, the binding energies of the neutral compounds in Table 7 are weakened with respect to those in the clusters without adsorbed oxygen (Table 1). The adsorption of OH to the oxygenated clusters is highly exothermic with only one exception, $O_2CrCrPt$, which has a positive binding energy of 0.6 eV. Interestingly, the CrCrPt cluster has a high affinity for atomic oxygen and for OH, in the absence of adsorbed molecular oxygen on the CrCr bridge site. However, once O_2 is adsorbed, the adsorption of OH on the remaining Pt site is not thermodynamically favorable. The attachment of two OH radicals to the same site is favorable in all cases, as shown by their large negative BEs.

TABLE 7: Binding Energies of One and Two OH to Oxygenated Metallic Clusters, O_2XYZ[a]

	−BE (eV)	
system	neutral	anion
$OH + O_2CoPtCo \rightarrow O_2CoPtCoOH$	3.51 (4.32)	5.92
$OH + O_2Co_2Pt \rightarrow O_2Co_2PtOH$	2.16 (2.88)	4.86
$2OH + O_2CoPtCo \rightarrow O_2CoPtCo(OH)_2$	7.90	10.44
$2OH + O_2Co_2Pt \rightarrow O_2Co_2Pt(OH)_2$	7.30	10.57
$OH + O_2Pt_2Co \rightarrow O_2Pt_2CoOH$	3.62 (3.56)	6.12
$OH + O_2PtCoPt \rightarrow O_2PtCoPtOH$	2.74 (2.94)	5.78
$2OH + O_2Pt_2Co \rightarrow O_2Pt_2Co(OH)_2$	8.32	10.72
$2OH + O_2PtCoPt \rightarrow O_2PtCoPt(OH)_2$	5.43	8.97
$OH + O_2Cr_2Pt \rightarrow O_2Cr_2PtOH$	−0.60 (3.32)	1.82
$OH + O_2CrPtCr \rightarrow O_2CrPtCrOH$	3.39	4.40
$2OH + O_2Cr_2Pt \rightarrow O_2Cr_2Pt(OH)_2$	4.23	6.51
$2OH + O_2CrPtCr \rightarrow O_2CrPtCr(OH)_2$	8.48	10.56
$OH + O_2PtCrPt \rightarrow O_2PtCrPtOH$	2.84 (2.90)	5.60
$OH + O_2Pt_2Cr \rightarrow O_2Pt_2CrOH$	3.64 (3.58)	6.21
$2OH + O_2PtCrPt \rightarrow O_2PtCrPt(OH)_2$	7.17	9.57
$2OH + O_2Pt_2Cr \rightarrow O_2Pt_2Cr(OH)_2$	8.72	11.13
$OH + O_2NiPtNi \rightarrow O_2NiPtNiOH$	3.19	5.73
$OH + O_2Ni_2Pt \rightarrow O_2Ni_2PtOH$	2.36 (2.74)	5.28
$2OH + O_2NiPtNi \rightarrow O_2NiPtNi(OH)_2$	8.36	10.60
$2OH + O_2Ni_2Pt \rightarrow O_2Ni_2Pt(OH)_2$	6.63	9.34
$OH + O_2NiPtPt \rightarrow O_2NiPtPtOH$	2.79	5.90
$OH + O_2PtPtNi \rightarrow O_2PtPtNiOH$	2.95	6.60
$2OH + O_2NiPtPt \rightarrow O_2NiPtPt(OH)_2$	6.31	9.35
$2OH + O_2PtPtNi \rightarrow O_2PtPtNi(OH)_2$	8.06	10.48

[a] In all cases, O_2 is adsorbed on the XY bridge site of the XYZ cluster, and the OH groups are adsorbed on top of the Z atomic site (geometry is depicted in Figure 1). The B3PW91 functional is used for all calculations with the LANL basis set and effective core potential for all atoms. Numbers in parentheses following the BE of neutral compounds are the corresponding BEs for the nonoxygenated clusters shown in Table 1.

TABLE 8: Absolute and Zero-Point Energies and Multiplicities at the B3PW91/LANL2DZ Level of Ground States for the Neutrals of the Systems in Table 7

system	*m*	energy (Ha)	ZPE (Ha)	energy + ZPE (Ha)
OH	2	−75.70353	0.00887	−75.69466
$O_2CoPtCo$	7	−559.69647	0.00636	−559.69011
O_2Co_2Pt	7	−559.74730	0.00686	−559.74044
O_2Pt_2Co	6	−533.76476	0.00581	−533.75895
$O_2PtCoPt$	6	−533.80297	0.00638	−533.79659
O_2Cr_2Pt	7	−442.32937	0.00777	−442.33714
$O_2PtCrPt$	3	−475.04450	0.00633	−475.05083
$O_2CrPtCr$	9	−442.17443	0.00611	−442.18054
O_2Pt_2Cr	7	−474.99771	0.00594	−475.00364
$O_2CoPtCoOH$	6	−635.52892	0.01831	−635.50620
O_2Co_2PtOH	6	−635.53028	0.01935	−635.51093
$O_2CoPtCo(OH)_2$	3	−711.39370	0.03286	−711.36084
$O_2Co_2Pt(OH)_2$	7	−711.42277	0.03456	−711.38821
O_2Pt_2CoOH	7	−609.60130	0.01892	−609.58238
$O_2PtCoPtOH$	5	−609.60717	0.01983	−609.58734
$O_2Pt_2Co(OH)_2$	6	−685.47768	0.03524	−685.44244
$O_2PtCoPt(OH)_2$	4	−685.40946	0.03407	−685.37539
O_2Cr_2PtOH	10	−518.01852	0.01876	−517.99977
$O_2CrPtCrOH$	2	−518.00877	0.01877	−517.99000
$O_2PtCrPtOH$	4	−550.85866	0.02017	−550.83849
O_2Pt_2CrOH	8	−550.84108	0.01901	−550.82207
$O_2Cr_2Pt(OH)_2$	3	−593.89973	0.03405	−593.86569
$O_2CrPtCr(OH)_2$	7	−593.89920	0.03350	−593.86570
$O_2PtCrPt(OH)_2$	5	−626.72130	0.03510	−626.68620
$O_2Pt_2Cr(OH)_2$	7	−626.73100	0.03462	−626.69638
$O_2NiPtNiOH$	2	−683.98298	0.01889	−683.96409
O_2Ni_2PtOH	6	−683.97953	0.01876	−683.96077
$O_2NiPtNi(OH)_2$	5	−759.87658	0.03451	−759.84207
$O_2Ni_2Pt(OH)_2$	5	−759.83974	0.03363	−759.80611

TABLE 9: Absolute and Zero-Point Energies and Multiplicities of Ground States for the Anions of the Systems in Table 7 at the B3PW91/LANL2DZ Level

system	*m*	energy (Ha)	ZPE (Ha)	energy + ZPE (Ha)
$O_2CoPtCoOH$	7	−635.61757	0.01861	−635.59896
O_2Co_2PtOH	7	−635.62939	0.01875	−635.61064
$O_2CoPtCo(OH)_2$	2	−711.48721	0.03212	−711.45509
$O_2Co_2Pt(OH)_2$	8	−711.54262	0.03370	−711.50892
O_2Pt_2CoOH	6	−609.69304	0.01805	−609.67499
$O_2PtCoPtOH$	4	−609.71893	0.01967	−609.69926
$O_2Pt_2Co(OH)_2$	5	−685.56592	0.03443	−685.53149
$O_2PtCoPt(OH)_2$	3	−685.53954	0.03138	−685.50816
O_2Cr_2PtOH	9	−518.10745	0.01861	−518.08884
$O_2CrPtCrOH$	3	−518.04591	0.01845	−518.02746
$O_2PtCrPtOH$	5	−550.96028	0.01927	−550.94102
O_2Pt_2CrOH	7	−550.93545	0.01830	−550.91716
$O_2Cr_2Pt(OH)_2$	2	−593.98333	0.03374	−593.94959
$O_2CrPtCr(OH)_2$	2	−593.97583	0.03223	−593.94360
$O_2PtCrPt(OH)_2$	4	−626.80971	0.03445	−626.77526
$O_2Pt_2Cr(OH)_2$	8	−626.81967	0.03421	−626.78546
$O_2NiPtNiOH$	5	−684.07624	0.01841	−684.05783
O_2Ni_2PtOH	5	−684.08657	0.01884	−684.05740
$O_2NiPtNi(OH)_2$	4	−759.95870	0.03528	−759.92342
$O_2Ni_2Pt(OH)_2$	4	−759.93950	0.03371	−759.90579

This multiple adsorption could also have important implications for the OER. Thus, studies are in progress to determine collective effects of multiple adsorptions of these intermediate species.

Table 7 also shows binding energies to a negatively charged O_2XYZ cluster. The purpose of this calculation was to investigate the effect of an applied field that would negatively charge the active sites on the OH adsorption. The results indicate that all the binding energies (including the case of $O_2CrCrPt$) are negative, i.e., thermodynamically favorable. To illustrate the geometries of the single and double adsorption of OH to an O_2XYZ (X, Y, Z is either Pt or Co) cluster, a characteristic geometry is depicted in Figure 1, and representative distances and angles are reported in Table 11.

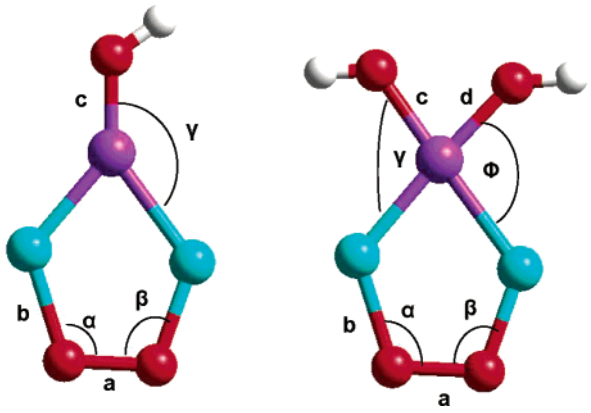

Figure 1. Geometries of an oxygenated cluster with one and two OH groups attached to the metal atom (O, red; H, white; metal atoms, purple and light blue spheres). The indicated notation for angles and distances is being used in Table 11.

TABLE 10: Energy Differences (in eV) between the Ground State and Higher-Energy States for Systems in Table 7

	m									
system	1	2	3	4	5	6	7	8	9	10
$O_2CoPtCoOH$		1.13		0.91		0.00		0.08		
O_2Co_2PtOH		0.21		0.67		0.00		0.18		1.81
$O_2CoPtCo(OH)_2$	3.33		0.00		0.82					
$O_2Co_2Pt(OH)_2$	1.17		1.29		0.61		0.00		2.11	
O_2Pt_2CoOH	2.16		0.81		0.85		0.00		1.5	
$O_2PtCoPtOH$	1.33		0.06		0.00		0.26		2.13	
$O_2Pt_2Co(OH)_2$		0.62		0.70		0.00		1.98		
$O_2PtCoPt(OH)_2$		1.61		0.00		0.10		0.40		
O_2Cr_2PtOH		2.65		2.64		1.29		0.03		0.00
$O_2CrPtCrOH$		0.00		0.41						
$O_2PtCrPtOH$		1.20		0.00		0.18				
O_2Pt_2CrOH		0.29		0.14		0.18		0.00		1.09
$O_2Cr_2Pt(OH)_2$			0.00		1.03					
$O_2CrPtCr(OH)_2$			2.37		1.03		0.00		0.07	
$O_2PtCrPt(OH)_2$	2.34		1.34		0.00		0.07			
$O_2Pt_2Cr(OH)_2$					0.01		0.00		1.65	
$O_2NiPtNiOH$		0.00		0.47		0.28				
O_2Ni_2PtOH		0.02		0.02		0.00		1.87		4.30
$O_2NiPtNi(OH)_2$	1.27		0.03		0.00		1.74			
$O_2Ni_2Pt(OH)_2$	1.38		0.15		0.00		1.78			
$O_2CoPtCoOH$	3.18		0.10		0.17		0.00		0.63	
O_2Co_2PtOH	2.77		0.54		0.32		0.00		1.16	
$O_2CoPtCo(OH)_2$		0.00		0.78		0.05		0.19		0.12
$O_2Co_2Pt(OH)_2$		1.57		2.07		1.54		0.00		1.58
O_2Pt_2CoOH		0.01		0.89		0.00		0.27		
$O_2PtCoPtOH$		0.58		0.00		0.19				
$O_2Pt_2Co(OH)_2$	2.27		0.48		0.00		0.98			
$O_2PtCoPt(OH)_2$	2.89		0.00		0.50		0.23			
O_2Cr_2PtOH					1.62		1.33		0.00	
$O_2CrPtCrOH$	3.27		0.00		0.70					
$O_2PtCrPtOH$			0.39		0.00		0.48			
O_2Pt_2CrOH							0.00		0.22	
$O_2Cr_2Pt(OH)_2$		0.00		1.29		1.68				
$O_2CrPtCr(OH)_2$		0.00		2.57		1.15		0.15		0.07
$O_2PtCrPt(OH)_2$		3.90		0.00		2.50				
$O_2Pt_2Cr(OH)_2$						0.10		0.00		0.39
$O_2NiPtNiOH$	1.19		0.10		0.00		0.70			
O_2Ni_2PtOH	1.03		0.31		0.00		1.56			
$O_2NiPtNi(OH)_2$		0.14		0.00		1.11				
$O_2Ni_2Pt(OH)_2$		0.27		0.00		1.51				

4. Conclusions

Calculated binding energies of O, OH, and H_2O to bimetallic clusters PtX, PtPtX, and PtXX (X = Pt, Co, Cr, Ni) show that the second metal element in the alloy has a stronger affinity for OH, O, and H_2O than the Pt sites. The highest binding strength of atomic oxygen is found in the hollow sites of Ni_3 and Co_3, followed by adsorption in hollow or bridge sites of PtPtX or PtXX, in all cases significantly stronger than in Pt_3.

TABLE 11: Distances and Angles of the Neutral (Table 8) and Anion (Table 9) Pt−Co Oxygenated Clusters with Geometries Depicted in Figure 1[a]

system	*a* (Å)	*b* (Å)	*c* (Å)	*d* (Å)	α (deg)	*β* (deg)	*γ* (deg)	Φ (deg)
$O_2CoPtCoOH$ (6)	1.488	1.834	1.762		109.1	102.8	116.2	
O_2Co_2PtOH (6)	1.481	1.819	1.945		108.3	107.9	129.7	
$O_2CoPtCo(OH)_2$ (3)	1.439	1.898	1.756	1.925	107.7	102.5	101.1	38.7
$O_2Co_2Pt(OH)_2$ (7)	1.486	1.795	2.056	2.056	114.1	113.9	46.4	46.4
O_2Pt_2CoOH (7)	1.374	2.142	1.760		106.7	106.5	147.0	
$O_2PtCoPtOH$ (5)	1.472	1.949	1.924		111.7	102.9	124.9	
$O_2Pt_2Co(OH)_2$ (6)	1.429	1.963	1.849	1.849	109.6	109.6	51.8	51.8
$O_2PtCoPt(OH)_2$ (4)	1.490	1.939	1.996	1.989	109.0	102.4	169.2	41.7
$O_2CoPtCoOH$ (7)	1.491	1.842	1.826		105.6	100.6	131.0	
O_2Co_2PtOH (7)	1.511	1.863	2.030		104.5	104.0	150.1	
$O_2CoPtCo(OH)_2$ (2)	1.519	1.806	1.789	1.934	103.8	103.1	101.6	39.2
$O_2Co_2Pt(OH)_2$ (8)	3.193	1.772	2.042	2.138	28.7	129.8	44.2	50.4
O_2Pt_2CoOH (6)	1.398	2.164	1.814		107.8	107.7	145.8	
$O_2PtCoPtOH$ (4)	1.489	2.121	1.995		107.1	100.2	127.5	
$O_2Pt_2Co(OH)_2$ (5)	1.457	1.968	1.908	1.908	108.0	108.0	49.2	49.2
$O_2PtCoPt(OH)_2$ (3)	1.487	1.934	1.961	3.475	108.5	107.9	166.1	31.1

[a] Multiplicities are indicated in parentheses after the compound stoichiometric formula.

H_2O adsorbs on the top sites of pure and alloy clusters with much weaker energies compared to those of OH and O; however, the H_2O binding strength in the Co, Cr, and Ni atoms is enhanced with respect to that on the Pt site, whereas the binding strength of H_2O on top of the Pt sites of the alloy clusters is much lowered with respect to that in the pure cluster. The bimetallic clusters are able to adsorb up to two OH radicals per site in oxygenated clusters, and their binding energies increase in negatively charged clusters.

In all cases, the foreign atom (Cr, Co, Ni) becomes highly oxidized by O, OH, and even by the water oxygen. The results suggest that the oxygen electroreduction current on Pt-based bimetallic surfaces would be increased in the presence of these atoms because of their ability to bind OH radicals and water and to "free" precious Pt atoms which would become readily available for further O_2 reduction. The differences between arrangements of atoms in specific bimetallic ensembles show the importance of geometric and electronic effects on the adsorption of intermediates of the oxygen electroreduction reaction.

Acknowledgment. This work is supported by the Department of Energy/Basic Energy Sciences, Grant DE-FG02-1ER15249. The use of computational facilities at the National Energy Research Scientific Computing Center and at the Major Shared Resource Center is gratefully acknowledged. J.M.S. acknowledges the University of South Carolina NanoCenter for financial support.

References and Notes

(1) Mukerjee, S.; Srinivasan, S.; Soriaga, M. P. Effect of Preparation Conditions of Pt Alloys on Their Electronic, Structural, and Electrocatalytic Activities for Oxygen Reduction-XRD, XAS, and Electrochemical Studies. *J. Phys. Chem.* **1995**, *99*, 4577

(2) Markovic, N. M.; Ross, P. N. Surface Science Studies of Model Fuel Cells Electrocatalysts. *Surf. Sci. Rep.* **2002**, *286*, 1

(3) Mukerjee, S.; Srinivasan, S. Enhanced electrocatalysis of oxygen reduction on platinum alloys in proton-exchange membrane fuel cells. *J. Electroanal. Chem.* **1993**, *357*, 201.

(4) Paulus, U. A.; Vokaun, A.; Scherer, G. G.; Schmidt, T. J.; Stamenkovic, V.; Markovic, N. M.; Ross, P. N. Oxygen reduction on high surface area Pt-based alloy catalysts in comparison to well defined smooth bulk alloy electrodes. *Electrochim. Acta* **2002**, *47*, 3787.

(5) Paulus, U. A.; Vokaun, A.; Scherer, G. G.; Schmidt, T. J.; Stamenkovic, V.; Radmilovic, V.; Markovic, N. M.; Ross, P. N. Oxygen reduction on carbon-supported Pt−Ni and Pt−Co alloy catalysts. *J. Phys. Chem. B* **2002**, *106*, 4181.

(6) Balbuena, P. B.; Altomare, D.; Agapito, L. A.; Seminario, J. M. Adsorption of oxygen on Pt-based clusters alloyed with Co, Ni, and Cr. *J. Phys. Chem. B* **2003**, *107*, 13671.

(7) Adzic, R. Recent advances in the kinetics of oxygen reduction. In *Electrocatalysis*; Lipkowski, J., Ross, P. N., Eds.; Wiley-VCH: New York, 1998; p 197.

(8) Sidik, R. A.; Anderson, A. B. Density functional theory study of O_2 electroduction when bonded to a Pt dual site. *J. Electroanal. Chem.* **2002**, *528*, 69.

(9) Wang, Y.; Balbuena, P. B. Ab initio-molecular dynamics studies of O_2 electroreduction on Pt (111): Effects of proton and electric field. *J. Phys. Chem. B* **2004**, *108*, 4376.

(10) Li, T.; Balbuena, P. B. Oxygen reduction on a platinum cluster. *Chem. Phys. Lett.* **2003**, *367*, 439.

(11) Damjanovic, A.; Brusic, V. Electrode kinetics of oxygen reduction on oxide-free platinum electrodes. *Electrochim. Acta* **1967**, *12*, 615.

(12) Markovic, N. M.; Ross, P. N. Electrocatalysis at well-defined surfaces: Kinetics of oxygen reduction and hydrogen oxidation/evolution on Pt(*hkl*) electrodes. In *Interfacial Electrochemistry. Theory, Experiment and Applications*; Wieckowski, A., Ed.; Marcel Dekker: New York, 1999; p 821.

(13) Calvo, S. R.; Mainardi, D. S.; Jansen, A. P. J.; Lukkien, J. J.; Balbuena, P. B. Test of a mechanism for O_2 electroreduction on Pt(111) via Dynamic Monte Carlo simulations. Meeting of the Electrochemical Society, 2003.

(14) Anderson, A. B. O_2 reduction and CO oxidation at the Pt-electrolyte interface. The role of H_2O and OH adsorption bond strengths. *Electrochim. Acta* **2002**, *47*, 3759.

(15) Ruban, A. V.; Skriver, H. L.; Norskov, J. K. Surface segregation energies in transition-metal alloys. *Phys. Rev. B* **1999**, *59*, 15990.

(16) Mainardi, D. S.; Balbuena, P. B. Surface Segregation in Bimetallic Nanoclusters: Geometric and Thermodynamic Effects. *Int. J. Quantum Chem.* **2001**, *85*, 580.

(17) Mainardi, D. S.; Balbuena, P. B. Monte Carlo Simulation Studies of Surface Segregation in Copper−Nickel Nanoclusters. *Langmuir* **2001**, *17*, 2047.

(18) Huang, S.-P.; Balbuena, P. B. Melting of bimetallic Cu−Ni nanoclusters. *J. Phys. Chem. B* **2002**, *106*, 7225.

(19) Huang, S.-P.; Mainardi, D. S.; Balbuena, P. B. Structure and dynamics of graphite-supported bimetallic nanoclusters. *Surf. Sci.* **2003**, *545*, 163.

(20) Balbuena, P. B.; Derosa, P. A.; Seminario, J. M. Density functional theory study of copper clusters. *J. Phys. Chem. B* **1999**, *103*, 2830.

(21) Derosa, P. A.; Balbuena, P. B.; Seminario, J. M. First-principles calculations on Cu and Cu−Ni clusters. AIChE Topical Conference: Applying molecular modeling and computational chemistry, Miami, FL, 1998.

(22) Mainardi, D. S.; Balbuena, P. B. Hydrogen and Oxygen Adsorption on Rhn ($n = 1-6$) Clusters. *J. Phys. Chem. A* **2003**, *107*, 10370.

(23) Li, T.; Balbuena, P. B. Computational studies of the interactions of oxygen with platinum clusters. *J. Phys. Chem. B* **2001**, *105*, 9943.

(24) Becke, A. D. Density-functional thermochemistry. III. The role of exact exchange. *J. Chem. Phys.* **1993**, *98*, 5648.

(25) Perdew, J. P.; Wang, Y. Accurate and simple analytic representation of the electron-gas correlation energy. *Phys. Rev. B* **1992**, *45*, 13244.

(26) Perdew, J. P.; Chevary, J. A.; Vosko, S. H.; Jackson, K. A.; Pederson, M. R.; Singh, D. J.; Fiolhais, C. Atoms, molecules, solids and surfaces: applciations of the generalized gradient approximation for exchange and correlation. *Phys. Rev. B* **1992**, *46*, 6671.

(27) Wadt, W. R.; Hay, P. J. Ab initio effective core potentials for molecular calculations. Potentials for main group elements Na to Bi. *J. Chem. Phys.* **1985**, *82*, 284.

(28) Hay, P. J.; Wadt, W. R. Ab initio effective core potentials for molecular calculations. Potentials for the transition metal atoms Sc to Hg. *J. Chem. Phys.* **1985**, *82*, 270.

(29) Hay, P. J.; Wadt, W. R. *J. Chem Phys.* **1985**, *82*, 299.

(30) Hehre, W. J.; Radom, L.; Schleyer, P. v. R.; Pople, J. A. *Ab Initio Molecular Orbital Theory*; John Wiley & Sons: New York, 1986.

(31) Perdew, J. P. Unified theory of exchange and correlation beyond the local density approximation. In *Electronic Structure of Solids*; Ziesche, P., Eschrig, H., Eds.; Akademie Verlag: Berlin, 1991.

(32) Seminario, J. M.; Tour, J. M. Ab initio methods for the study of molecular systems for nanometer technology. In *Molecular electronics: science and technology*; Aviram, A., Ratner, M., Eds.; Annals of the NY Academy of Sciences: New York, 1998.

(33) Seminario, J. M.; Zacarias, A. G.; Tour, J. M. Theoretical study of a molecular tunneling diode. *J. Am. Chem. Soc.* **2000**, *122*, 3015.

(34) Frisch, M. J.; Trucks, G. W.; Schlegel, H. B.; Scuseria, G. E.; Robb, M. A.; Cheeseman, J. R.; Zakrzewski, V. G.; Montgomery, J. A., Jr.; Stratmann, R. E.; Burant, J. C.; Dapprich, S.; Millam, J. M.; Daniels, A. D.; Kudin, K. N.; Strain, M. C.; Farkas, O.; Tomasi, J.; Barone, V.; Cossi, M.; Cammi, R.; Mennucci, B.; Pomelli, C.; Adamo, C.; Clifford, S.; Ochterski, J.; Petersson, G. A.; Ayala, P. Y.; Cui, Q.; Morokuma, K.; Malick,

D. K.; Rabuck, A. D.; Raghavachari, K.; Foresman, J. B.; Cioslowski, J.; Ortiz, J. V.; Stefanov, B. B.; Liu, G.; Liashenko, A.; Piskorz, P.; Komaromi, I.; Gomperts, R.; Martin, R. L.; Fox, D. J.; Keith, T.; Al-Laham, M. A.; Peng, C. Y.; Nanayakkara, A.; Gonzalez, C.; Challacombe, M.; Gill, P. M. W.; Johnson, B. G.; Chen, W.; Wong, M. W.; Andres, J. L.; Head-Gordon, M.; Replogle, E. S.; Pople, J. A. *Gaussian 98*, revision A.11; Gaussian, Inc.: Pittsburgh, PA, 1998.

(35) Bedurftig, K.; Volkening, S.; Wang, Y.; Wintterlin, J.; Jacobi, K.; Ertl, G. Vibrational and structural properties of OH adsorbed on Pt(111). *J. Chem. Phys.* **1999**, *111*, 11147.

(36) Michaelides, A.; Hu, P. A density functional theory study of hydroxyl and the intermediate in the water formation reaction on Pt. *J. Chem. Phys.* **2001**, *114*, 513.

(37) Fisher, G. B.; Sexton, B. A. Identification of an adsorbed hydroxyl species on the Pt(111) surface. *Phys. Rev. Lett.* **1980**, *44*, 683.

(38) Gilarowski, G.; Erley, W.; Ibach, H. Photochemical reactions of water adsorbed on Pt(111). *Surf. Sci.* **1996**, *351*, 159.

(39) Koper, M. T. M.; Shubina, T. E.; Santen, R. A. v. Periodic density functional study of CO and OH adsorption on Pt−Ru alloy surfaces: Implications for CO tolerant fuel cell catalysts. *J. Phys. Chem. B* **2002**, *106*, 686.

(40) Mulliken, R. S. Electronic population analysis on LCAO-MO molecular wave functions. I. *J. Chem. Phys.* **1955**, *23*, 1833.

(41) Mulliken, R. S. Electronic population analysis on LCAO-MO molecular wave functions. III Effects of hybridization on overlap and gross AO populations. *J. Chem. Phys.* **1955**, *23*, 2338.

(42) Mulliken, R. S. Electronic population analysis on LCAO-MO molecular wave functions. II. Overlap populations, bond orders, and covalent bond energies. *J. Chem. Phys.* **1955**, *23*, 1841.

(43) Jacob, T.; Merinov, B. V.; Goddard, W. A. Chemisorption of atomic oxygen on Pt(111) and Pt/Ni(111) surfaces. *Chem. Phys. Lett.* **2004**, *385*, 374.

(44) Gland, J. L.; Sexton, B. A.; Fisher, G. B. Oxygen interactions with the Pt (111) surface. *Surf. Sci.* **1980**, *95*, 587.

(45) Gland, J. L. Molecular and atomic adsorption of oxygen on the Pt (111) and Pt (S)-12 (111) × (111) surfaces. *Surf. Sci.* **1980**, *93*, 487.

(46) Campbell, C. T.; Ertl, G.; Kuipers, H.; Segner, J. A molecular beam study of the adsorption and desorption of Oxygen from a Pt (111) Surface. *Surf. Sci.* **1981**, *107*, 220.

(47) Meng, S.; Xu, L. F.; Wang, E. G.; Gao, S. Vibrational recognition of hydrogen-bonded water networks on a metal surface. *Phys. Rev. lett.* **2002**, *89*, 176104.

(48) Ogasawara, H.; Brena, B.; Nordlund, D.; Nyberg, M.; Pelmenschikov, A.; Pettersson, L. G. M.; Nilsson, A. Structure and bonding of water on Pt(111). *Phys. Rev. Lett.* **2002**, *89*, 276102.